Photofragment fluorescence polarization following photolysis of $HgBr_2$ at 193 nm[a]

J. Husain,[b] J. R. Wiesenfeld,[c] and R. N. Zare

Department of Chemistry, Stanford University, Stanford, California 94305
(Received 6 September 1979; accepted 7 November 1979)

When $HgBr_2$ (2–45 mTorr) is photolyzed by the linearly polarized output of an ArF excimer laser (193 nm), the visible emission from the HgBr $B\,^2\Sigma^+$ fragment is found to be linearly polarized. The degree of polarization is $11.9\% \pm 1.5\%$, in close agreement with the theoretical value of 14.3% predicted for a $^1\Sigma_g^+(^1A_1) \rightarrow {}^1B_2(^1\Sigma_u^+)$ dissociative transition in $HgBr_2$. The addition of inert gases depolarizes the HgBr* emission. A simple model, developed to calculate the average angle through which the angular momentum vector of the HgBr* fragment is tipped by each hard sphere collision, fits well the pressure dependence of the depolarization.

I. INTRODUCTION

Photolysis of isolated molecules continues to play a significant role in the development of dissociation dynamics because such processes may be examined by a variety of experimental techniques and the results of these studies appear to be amenable to relatively straightforward theoretical treatment.[1,2] Recently it has been suggested that the observation of polarized emission from excited photofragments may provide an appealing alternative, when applicable, to the measurement of photofragment angular distributions in learning about the symmetry of the repulsive state responsible for dissociation.[3–5] The polarization of diatomic emission from photodissociation of a triatomic molecule has been observed following vacuum ultraviolet photolysis of H_2O[4,6] D_2O,[6] HCN,[7] BrCN,[7,8] and ICN.[8,9] Unfortunately, while present theory[5] is restricted to direct photodissociation, all of the above molecular systems involve fragmentation from predissociating excited states. Consequently, previous experiments have not been able to test the predicted value of the degree of polarization.

In this study we report measurements on the degree of polarization of the HgBr($B\,^2\Sigma^+ - X\,^2\Sigma^+$) emission following the photolysis of $HgBr_2$ by the 193 nm output of an argon fluoride (ArF) laser. The resulting polarization is shown to be in substantial agreement with theory, permitting the identification of the symmetry nature of the dissociative state. We also present a study of the collisional depolarization of this emission. A simple model is proposed to account for the observed behavior.

II. EXPERIMENTAL

Figure 1 illustrates the experimental setup. The 193 nm output of an ArF excimer laser is incident on a sample of $HgBr_2$ vapor contained in a heated Pyrex cell. The resulting blue-green emission, HgBr $B\,^2\Sigma^+ \rightarrow X\,^2\Sigma^+$, is monitored perpendicular to the direction of the laser beam by a photomultiplier. Polarization analyzers are placed in front of the detector and permit the measurement of $I_\parallel$ and $I_\perp$, the intensities of the fluorescence polarized parallel and perpendicular, respectively, to the electric vector of the laser beam. The degree of polarization, P, is calculated from the expression

$$P = \frac{I_\parallel - I_\perp}{I_\parallel + I_\perp} , \tag{1}$$

Details of the experimental apparatus and the measurement procedure follow.

A. Photolysis source

The excimer laser was built previously by Z. Karny in this laboratory. It is capable of producing 193 nm pulses, of 20 nsec in duration, with 8–12 mJ energy at 1 Hz. This is sufficient to observe intense HgBr B–X emission at relatively low vapor pressures of $HgBr_2$ (10^{-3}–10^{-2} Torr).

The excimer laser has synthetic quartz windows mounted at Brewster's angle. Thus the output is expected to be polarized, although the high gain of ArF may reduce the degree of polarization. In order to enhance the polarization of the laser output, two additional windows were placed at Brewster's angle inside the laser cavity. Using a MgF_2 Rochon polarizer (Karl Lam-

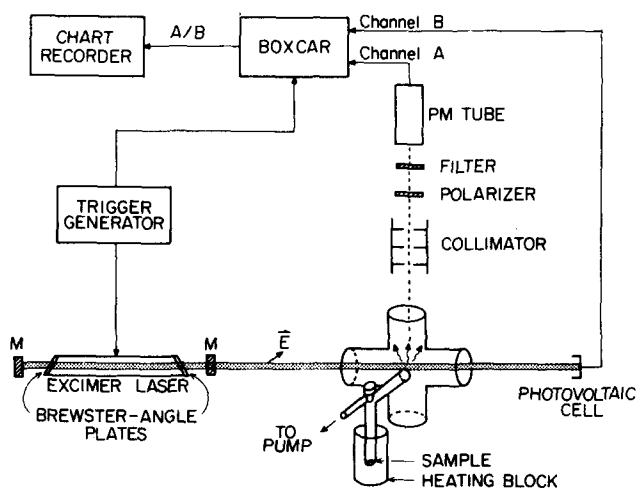

FIG. 1. Schematic diagram of the experimental apparatus.

[a]Supported in part by the Office of Naval Research under Contract N00014-78-C-0132 and the National Science Foundation under Grant NSF PHY 79-08694.
[b]Present address: Department of Physics, University of Missouri-Rolla, Rolla, MO 65401.
[c]On sabbatic leave. Permanent address: Department of Chemistry, Cornell University, Ithaca, NY 14853.

 0021-9606/80/042479-05$01.00

brecht Model RQ-12-1) the linear polarization of the 193 nm output is measured to be $92.3\% \pm 5.6\%$, indicating that the photolysis source is highly polarized but fluctuates from shot to shot. The observed polarizations are corrected for the partial polarization of the laser. If the incident beam were totally unpolarized, then the degree of polarization would be given by $P/(2-P)$, where P is the value for a totally polarized beam.[10] Thus the observed degree of polarization, P_{obs}, obtained using the present partially polarized beam may be related to P by

$$P_{obs} = 0.923P + 0.077P/(2-P) \quad , \tag{2}$$

Once P_{obs} is determined, then P may be found by solving the above quadratic equation (for which only one of its two roots is physically reasonable).

B. Sample preparation

The fluorescence cell is a Pyrex cross formed by the intersection of two cylinders 2.5 cm in diameter and 8 cm in length. Synthetic quartz windows are affixed to the cell with epoxy cement. The cell is painted black on the outside to minimize scattered light.

The $HgBr_2$ sample (Ventron, Alpha Division, >97% purity) is placed in a Pyrex coldfinger attached to the cell body. The cell is evacuated and any residual $HgBr_2$ in the cell body is sublimed into the coldfinger. The $HgBr_2$ vapor pressure is controlled by inserting the coldfinger into a brass block, which was wrapped with heating tape. The temperature of the block is controlled to ± 0.5 °C over the range 29–63 °C simply by use of a Variac autotransformer. The body of the cell is similarly wrapped with heating tape and the temperature maintained about 10 °C higher than the coldfinger to prevent condensation of $HgBr_2$ on the windows. The latter were encased in copper extension tubes to minimize cooling.

Cell degassing and sample preparation are carried out on a standard vacuum line (3×10^{-6} Torr base pressure). For experiments involving collisional depolarization by foreign gases, the cell is connected to the vacuum line by a short length of flexible polyethylene tubing evacuable to about 10^{-3} Torr. This is sufficient to ensure that possible impurities do not interfere with the observation of collisional effects by the added gases in the pressure range 0.1–100 Torr. The foreign gases studied are helium (Liquid Carbonic, 99.9999% purity) and krypton (Matheson, 99.995% purity).

C. Detection system

The HgBr fluorescence is detected with a photomultiplier (RCA 8850), the anode of which is connected across a 47 $k\Omega$ resistor. A 13 cm long series of baffles collimates the fluorescence so that the photomultiplier views the cell with an acceptance angle of less than 4°. A filter (Corning 4-67) is placed directly in front of the photomultiplier to isolate the 400–570 nm region. Fluorescence from the HgBr B state peaks near 500 nm. A polarization analyzer consisting of two sheet polarizers (Polaroid HN-32) side by side in a sliding mount is placed in front of the filter. The axes of the sheet polarizers are crossed and the extinction ratio is better than 10^{-3}. No discernible difference is detected when the axes of the sheet polarizers are reversed.

The output of the photomultiplier is fed into channel A of a boxcar integrator (PAR model 162). The opening of the gate is offset from the laser pulse to avoid contributions from electrical interference and scattered light. To take into account fluctuations in the laser intensity, typically 20%, the output of a photocell mounted on the laser beam axis behind the fluorescence cell is fed into channel B of the same boxcar. The A/B ratio of the fluorescence signal to the laser energy is averaged with a time constant corresponding to twenty laser shots and displayed on a stripchart recorder. By sliding the two sheet polarizers back and forth, $I_\parallel$ and $I_\perp$ are obtained. Typically $I_\parallel$ and $I_\perp$ are each recorded for 600 sec. Nevertheless, fluctuations in the shot to shot stability of the laser energy and its polarization constitute the major source of statistical uncertainty in the measured values of P.

III. RESULTS

A. Photofragment polarization

The degree of linear polarization of the HgBr $B^2\Sigma^+ \rightarrow X^2\Sigma^+$ emission following photodissociation of $HgBr_2$ is measured over the temperature range 29–63 °C, corresponding[11] to 6×10^{13} to 1×10^{15} $HgBr_2$ molecules per cm^3. The value of P is found to be constant, within experimental error, over this range of $HgBr_2$ density. This demonstrates that collisional depolarization of $HgBr(B^2\Sigma^+)$ with $HgBr_2$ is insignificant in these experiments. It should also be noted that the HgBr fluorescence has a uniform spatial distribution along the laser light path in the fluorescence cell. Even at a density as high as 3×10^{15} molecules per cm^3 the optical depth[12] of $HgBr_2$ at 193 nm is about 30 cm. The mean degree of linear polarization obtained by averaging all observed measurements is $P = 11.5\% \pm 1.1\%$, where the uncertainty represents 1 std. dev. When this result is corrected with the help of Eq. (2) for the partial degree of polarization of the laser we obtain the value

$$P = 11.9\% \pm 1.5\% \quad . \tag{3}$$

Because the radiative lifetime[13] of the HgBr B state is so short (23.7 nsec) no correction need be applied for depolarization in the earth's magnetic field.[14] The result of Eq. (3) is in close conformity with the theoretical value,[5] $P = 14.3\%$ ($P = \frac{1}{7}$).

Many checks were made to confirm this observed effect. The signal disappears when no $HgBr_2$ is in the fluorescence cell or when the fluorescence cell is not heated. Moreover, the degree of polarization essentially vanishes, $P = 1.2\% \pm 1.5\%$, when the direction of observation is chosen to be along the electric vector of the laser beam. Finally, as is demonstrated by the collisional depolarization studies described below, addition of foreign gas causes the polarization to decrease monotonically with increasing pressure.

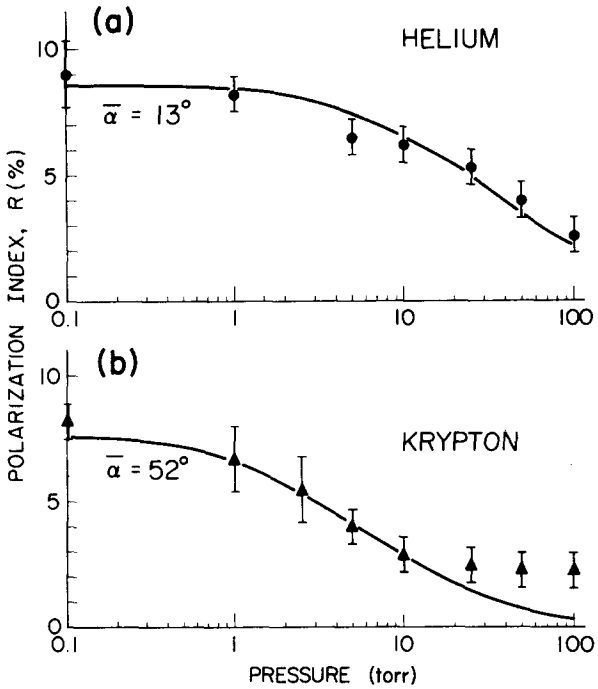

FIG. 2. Polarization index as a function of added foreign gas for (a) helium and (b) krypton. The solid lines are theoretical curves, based on a model in which each hard sphere collision tilts the plane of rotation of the diatomic emitter by the angle $\bar{\alpha}$ [see Eq. (11)].

B. Collisional depolarization

Figure 2 presents the polarization index

$$R=\frac{I_{\parallel}-I_{\perp}}{I_{\parallel}+2I_{\perp}} \tag{4}$$

as a function of foreign gas pressure for helium [Fig. 2(a)] and krypton [Fig. 2(b)]. The polarization index R may be related to the degree of polarization P by

$$R=\frac{2P}{3-P} \tag{5}$$

It is convenient to use the polarization index because the theory of collisional depolarization[15] is expressed more simply in terms of R than P. Note that the relative uncertainty in R increases at higher pressures as its magnitude diminishes. We also plot on Fig. 2 theoretical curves which will be discussed below (Sec. IV B). Comparison of Fig. 2(a) with 2(b) shows that depolarization is more marked for the heavier rare gas collision partner at the same pressure.

IV. DISCUSSION

A. Symmetry of the dissociative state

The mercury dihalides may be regarded formally as 16 valence electron systems, like CO_2. Then according to Walsh's rules,[16] the ground state is linear while the lowest-lying excited states are bent. Recent *ab initio* calculations[17] on $HgCl_2$ and $HgBr_2$ support this simple interpretation. In a linear – bent transition, the absorption transition dipole moment μ_{abs} may be either in the molecular plane or perpendicular to it. The incident radiation preferentially selects different $HgBr_2$ orientations according to the interaction $(\mu_{abs}\cdot\mathcal{E})^2$, where $\mathcal{E}$ is the electric vector of the plane polarized light beam. In direct photodissociation, the Br and HgBr* fragments separate on a time scale short compared to the rotational period of the $HgBr_2$* molecules. Moreover, the change in equilibrium geometry for a linear – bent transition causes the HgBr* to be rotationally excited, the extent of rotational excitation usually being larger than the thermal rotational excitation of the $HgBr_2$ parent.[1] Thus, because the forces between the recoiling Br and HgBr* fragments are directed in the plane of the HgBr* molecule, the rotational angular momentum J of the HgBr* fragment is not randomly distributed in space but lies perpendicular to the $HgBr_2$* molecular plane. This anisotropic J distribution causes the HgBr* emission to be polarized.

A simple classical theory has been developed to account for this effect.[5] A measurement of the degree of polarization combined with a knowledge of the transition dipole moment of the emitter gives the direction of μ_{abs}. For the HgBr B–X system, the emission transition dipole moment is along the internuclear axis (parallel-type transition), and theory predicts a value of $P=\frac{1}{7}$ if μ_{abs} lies in the molecular plane. Thus, if we assume $D_{\infty h}$ symmetry for the ground state and C_{2v} symmetry for the excited state, the dissociative transition is from the $^1\Sigma_g^+(^1A_1)$ ground state of $HgBr_2$ to a $^1B_2(^1\Sigma_u^+)$ excited state since for this type of transition μ_{abs} lies in the molecular plane. This conclusion is in agreement with the calculations by Wadt[17] on $HgBr_2$ where it is shown that the $^1B_2(^1\Sigma_u^+)$ excited state is the lowest excited state that correlates with $HgBr(B^2\Sigma^+)+Br(^2P)$. Thus we are able to identify the symmetry of the dissociative state of the mercury dihalides responsible for mercury monohalide laser action.[18–23]

B. The average tipping angle for collisional depolarization

The following treatment follows in the spirit of the work of Gordon.[15] It may be shown that for a single collision the polarization index R_1 can be related to its collisionless initial value R_0 by

$$R_1=R_0\langle P_2(\cos\alpha)\rangle \ , \tag{6}$$

where $\langle\rangle$ denotes the ensemble average over all possible collisions, $P_2(\cos\alpha)=(3\cos^2\alpha-1)/2$ is a Legendre polynomial of the second order, and α is the angle through which the angular momentum vector J of the diatomic molecule is tipped by a collision.[24,25] We introduce the approximation that each collision tips J by the same angle $\bar{\alpha}$, irrespective of the change in the magnitude of J, i.e., $\langle P_2(\cos\alpha)\rangle=P_2(\cos\bar{\alpha})$. We also assume that successive collisions are uncorrelated. Then the value of R after n collisions, represented as R_n, is related to R_0 by

$$R_n=R_0[P_2(\cos\bar{\alpha})]^n \ . \tag{7}$$

We denote the collision rate by τ_C^{-1} (where τ_C is the average time between collisions) and the spontaneous emission rate by τ_R^{-1} (where τ_R is the radiative lifetime). The normalized probability for an excited molecule to

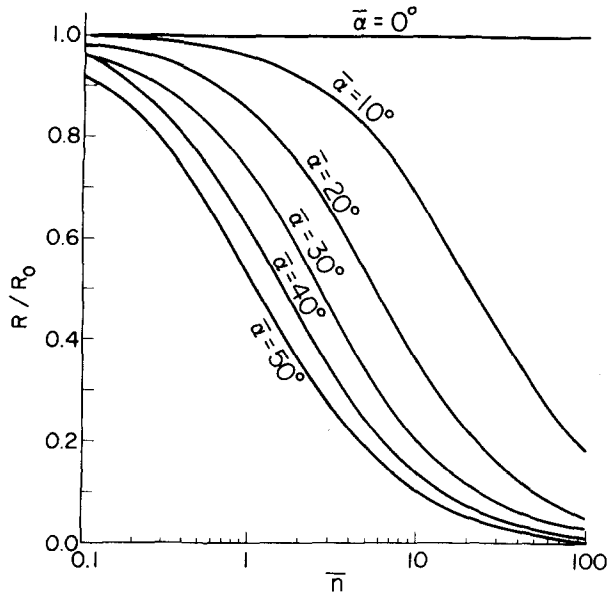

FIG. 3. The depolarization ratio, R/R_0, as a function of the average number of collisions, $\bar{n}$, for different tipping angles $\bar{\alpha}$.

make n collisions before it radiates is readily shown to be given by

$$p_n = (\bar{n})^n/(\bar{n}+1)^{n+1} \quad , \tag{8}$$

where

$$\bar{n} = \tau_C^{-1}/\tau_R^{-1} \tag{9}$$

is the average number of collisions.[26] Hence the observed polarization index R is obtained by averaging R_n over the collisions n:

$$R = \sum_n p_n R_n \quad . \tag{10}$$

This geometrical series has the sum

$$R = R_0 \frac{1}{1+\bar{n}(\frac{3}{2}\sin^2\bar{\alpha})} \quad . \tag{11}$$

Equation (11) represents the pressure dependence of the polarization index expressed in terms of the average number of collisions $\bar{n}$ and the tipping angle $\bar{\alpha}$. Figure 3 presents the family of curves of R/R_0 vs $\bar{n}$ for different values of $\bar{\alpha}$. It is seen that the depolarization ratio falls monotonically for all values of $\bar{\alpha}$ where $\bar{\alpha}$ ranges from 0° (no depolarization) to the magic angle, 54.7°, where a single collision causes complete depolarization ($R_1 = 0$). The above model predicts that one parameter, $\bar{\alpha}$, is sufficient to describe the pressure dependence of the depolarization. This treatment has neglected collisional quenching of the electronically excited molecule. For collisions with rare gas atoms this omission is expected to be valid at low pressures. However, in the more general case collisional quenching must be included in Eq. (11) which is an easy task to carry out.[27]

Our result may be compared to the expression obtained by Gordon[15] (when quenching is ignored)

$$R = R_0 \frac{1}{1+\rho\langle v\rangle\tau_R\sigma_{\text{pol}}} \quad , \tag{12}$$

where ρ is the number density of scatterers, $\langle v\rangle$ the relative velocity, and σ_{pol} is the reorientation cross section defined by

$$\sigma_{\text{pol}} = \int_0^\infty \frac{\langle v(\frac{3}{2}\sin^2\alpha)\rangle}{\langle v\rangle} 2\pi b db \quad , \tag{13}$$

where the integration is over all impact parameters b. We relate the collision rate τ_C^{-1} to the collision cross section σ_C by

$$\tau_C^{-1} = \rho\langle v\rangle\sigma_C \quad . \tag{14}$$

Then Eq. (11) becomes the same as Eq. (12) if we make the identification

$$\sigma_{\text{pol}} = (\tfrac{3}{2}\sin^2\bar{\alpha})\sigma_C \quad . \tag{15}$$

On comparing Eq. (15) to Eq. (13) we see that our model assumes that $\langle v\,\frac{3}{2}\sin^2\alpha\rangle/\langle v\rangle$ may be replaced by $\frac{3}{2}\sin^2\bar{\alpha}$, which is independent of the impact parameter.

The curves in Fig. 2 are calculated from Eq. (11) using the data given in Table I to estimate the hard sphere collision rate. The fit is good except for krypton at pressures near 100 Torr, where electronic quenching may become significant.[28] We find for helium that $\bar{\alpha} = 13°$ whereas for krypton $\bar{\alpha} = 52°$. The hard sphere cross sections for collisions of He and Kr with HgBr* are poorly characterized, and changes in their values will

TABLE I. Information for calculating hard sphere cross sections.

Collision partner	$\langle v\rangle$ [a]	r(HgBr)* [b]	r (Collision partner)[c]	σ_C [d]
He	1.33×10^5 cm/sec	26.1×10^{-9} cm	3.0×10^{-9} cm	2.66×10^{-15} cm^2
Kr	4.58×10^4 cm/sec	26.1×10^{-9} cm	8.5×10^{-9} cm	3.76×10^{-15} cm^2

[a]The velocity of the (HgBr)* fragment is computed to be 3.6×10^4 cm/sec based on the known value (3.06 eV) of the $HgBr_2$ dissociation energy (JANAF Thermochemical Tables, 2nd ed., D. R. Stull, H. Prophet, *et al.*, Project Directors, Natl. Stand. Ed. Data Ser. Natl. Bur. Stand. (1971)] and the energy of the 193 nm photon (6.40 eV). The average thermal velocities of the helium and krypton atoms are 1.28×10^5 and 2.70×10^4 cm/sec, respectively. The relative velocity $\langle v\rangle$ is computed assuming that the velocities of the two collision partners ane perpendicular.

[b]Taken from the calculation of W. R. Wadt, Appl. Phys. Lett. **34**, 658 (1979).

[c]Taken from S. Fraga, J. Karwowski, and K. M. S. Saxena, *Handbook of Atomic Data* (Elsevier, New York, 1976).

[d]Calculated from $\pi(r_1 + r_2)^2$.

cause corresponding changes in $\bar{\alpha}$. Nevertheless, our data indicate that a single collision between Kr and HgBr* causes almost complete reorientation of the latter.

ACKNOWLEDGMENTS

We are grateful to W. R. Wadt for useful discussions concerning the electronic structure of the bound and repulsive states of the mercury dihalides and to R. Bersohn for a critical reading of the first draft of this paper.

[1]J. P. Simons, *The Dynamics of Photodissociation*, in Gas Kinetics and Energy Transfer, Vol. 2, edited by P. G. Ashmore and R. J. Donovan, Chem. Soc. Spec. Per. Rep. (1977).
[2]W. M. Gelbart, "Photodissociation dynamics of polyatomic molecules," Ann. Rev. Phys. Chem. 28, 323 (1977).
[3]R. J. Van Brunt and R. N. Zare, J. Chem. Phys. **48**, 4304 (1968).
[4]G. A. Chamberlain and J. P. Simons, Chem. Phys. Lett. **32**, 355 (1975).
[5]M. T. MacPherson, J. P. Simons, and R. N. Zare, Mol. Phys. (in press).
[6]M. T. MacPherson and J. P. Simons, Chem. Phys. Lett. **51**, 261 (1977).
[7]G. A. Chamberlain and J. P. Simons, J. Chem. Soc. Faraday II **71**, 2043 (1975).
[8]M. T. MacPherson and J. P. Simons, J. Chem. Soc. Faraday II 75, 1572 (1979).
[9]E. D. Poliakoff, S. H. Southworth, D. A. Shirley, K. Jackson, and R. N. Zare, Chem. Phys. Lett. 65, 407 (1979).
[10]P. P. Feofilov, *The Physical Basis of Polarized Emission* (Consultants Bureau, New York, 1961), pp. 39–40; B. I. Stepanov and V. P. Gribkovskii, *Theory of Luminescence* (Iliffe, London, 1968), pp. 52–53.
[11]*CRC Handbook of Chemistry and Physics*, 59th ed. (Cleveland Rubber, West Palm Beach, 1978).
[12]J. Maya, J. Chem. Phys. **67**, 4976 (1977).
[13]R. W. Wayant and J. G. Eden, App. Phys. Lett. **33**, 708 (1978).
[14]See R. N. Zare, Acc. Chem. Res. **4**, 361 (1971).
[15]R. G. Gordon, J. Chem. Phys. **45**, 1643 (1966).
[16]A. D. Walsh, J. Chem. Soc. **2260** (1953).
[17]W. R. Wadt, J. Chem. Phys. 72, 2469 (1980), preceding paper. We are grateful to Wadt for sharing his results with us prior to publication.
[18]J. H. Parks, Appl. Phys. Lett. **31**, 192 (1977).
[19]J. H. Parks, Appl. Phys. Lett. **31**, 297 (1977).
[20]J. G. Eden, Appl. Phys. Lett. **31**, 448 (1977).
[21]W. T. Whitney, Appl. Phys. Lett. **32**, 239 (1978).
[22]E. J. Schimitschek, J. E. Celto, and J. A. Trias, Appl. Phys. Lett. **31**, 608 (1978).
[23]E. J. Schimitschek and J. E. Celto, Opt. Lett. **2**, 64 (1978).
[24]P. Soleillet, Ann. Phys. (Paris) **12**, 23 (1929); F. Perrin, J. Phys. Radium **7**, 390 (1926); Ann. Phys. **12**, 169 (1929).
[25]R. G. Gordon, J. Chem. Phys. **44**, 228, 3083 (1966).
[26]See T. Carrington, *Eighth Symposium (International) on Combustion* (Williams & Wilkins, Baltimore, 1962). This result may be derived simply as follows: Those molecules having undergone n and only n collision up to time t obey a Poisson distribution, i.e., $[(t\tau_C^{-1})^n/n\ ]\exp(-t\ \tau_C^{-1})$. The probability that such a molecule radiates between t and $t+dt$ is τ_R^{-1} $\times\exp(-t\ \tau_R^{-1})\ [(t\ \tau_C^{-1})^n/n\ ]\exp(-t\ \tau_C^{-1})dt$ and the probability p_n of a molecule making n collisions before radiating is

$$p_n=\frac{\tau_R^{-1}\ (\tau_C^{-1})^n}{n}\int_0^\infty t^n\exp[-t(\tau_R^{-1}+\tau_C^{-1})]dt\ ,$$

which leads to Eq. (8). Note that $\sum_n p_n=1$ and that $\sum_n n\,p_n$ $=\bar{n}=\tau_C^{-1}/\tau_R^{-1}$.
[27]Let the rate of collisional quenching be denoted by τ_Q^{-1}. Then the expression for the average number of collisions, $\bar{n}$, becomes $\bar{n}=\tau_C^{-1}/(\tau_R^{-1}+\tau_Q^{-1})$. With this generalization Eqs. (9) and (11) are valid as written. Note that Fig. 3 is still applicable but that $\bar{n}$ has a weaker than linear dependence on pressure when collisional quenching is present. This causes the depolarization ratio R/R_0 to be larger at a given pressure than would be expected if quenching is ignored.
[28]The data can be approximately fit by assuming τ_Q^{-1} is ~ 0.15 τ_C^{-1} and retaining the same value of $\bar{\alpha}$.